Electronic Supplementary Material (ESI) for Inorganic Chemistry Frontiers.

Supporting Information

Tailoring Energy Level and Surface Basicity of Metal Oxide Semiconductor by Rare-Earth Incorporation for High Performance Formaldehyde Detection

Yanfang Zhao,[a] Xiaoxin Zou,[a] Hui Chen,[a] Xuefeng Chu,[b] Guo-Dong Li*,[a]

[a] State Key Laboratory of Inorganic Synthesis and Preparative Chemistry, College of Chemistry, Jilin University, Changchun 130012, P. R. China

[b] Key Laboratory of Architectural Cold Climate Energy Management, Ministry of Education, Jilin Jianzhu University, Changchun 130118, China

* Corresponding author. E-mail address: lgd@jlu.edu.cn

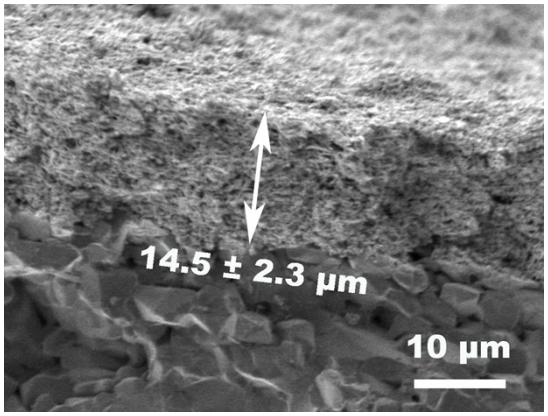

Figure S1 The thickness of the sensing film was measured by SEM.

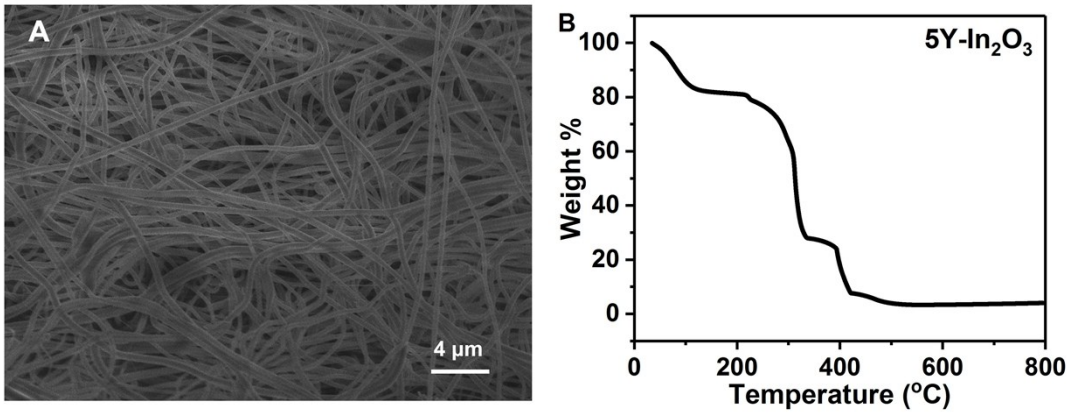

Figure S2 (A) SEM image and (B) Thermogravimetric (TG) curve of as prepared nanofiber precursor containing Y, In and PVP.

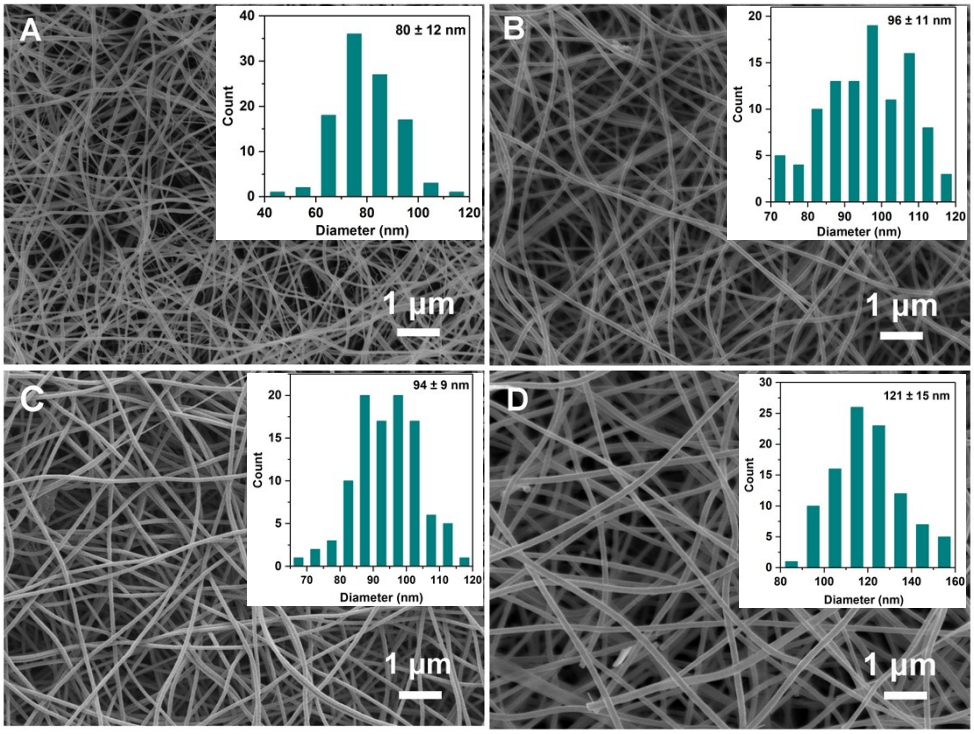

Figure S3 SEM images and corresponding nanofibers size-distribution diagrams of (A) In_2O_3, (B) 1Y-In_2O_3, (C) 3Y-In_2O_3 and (D) 7Y-In_2O_3.

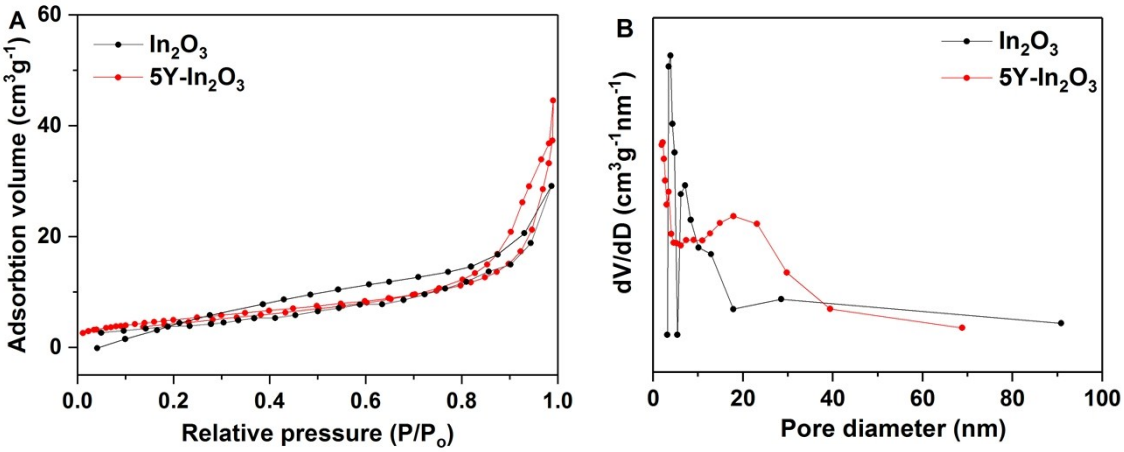

Figure S4 (A) N_2 adsorption-desorption isotherms and (B) pore size distribution curves of In_2O_3 and 5Y-In_2O_3.

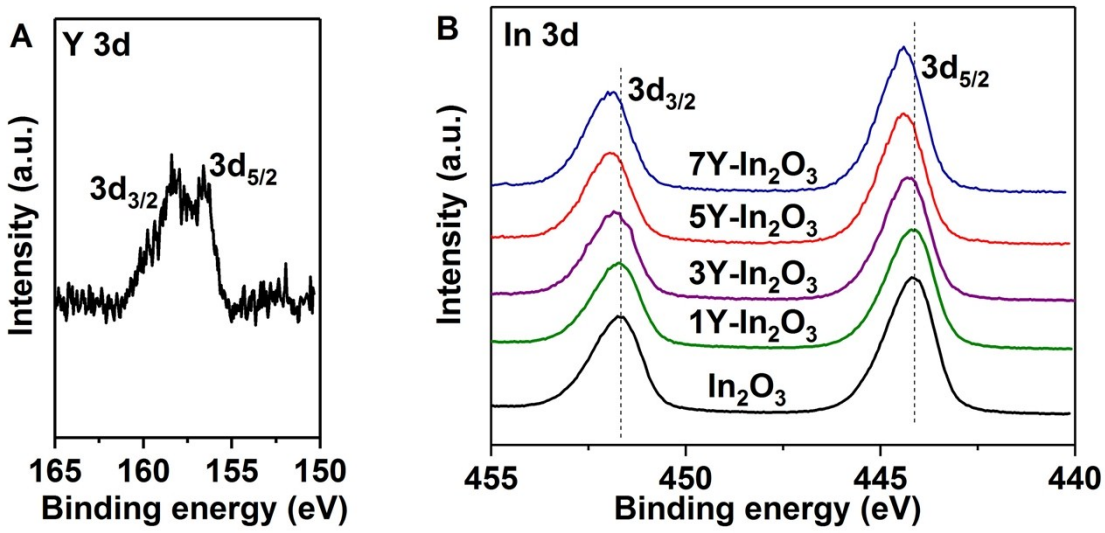

Figure S5 XPS of (A) Y 3d for 5Y-In_2O_3 and (B) In 3d for x Y-In_2O_3.

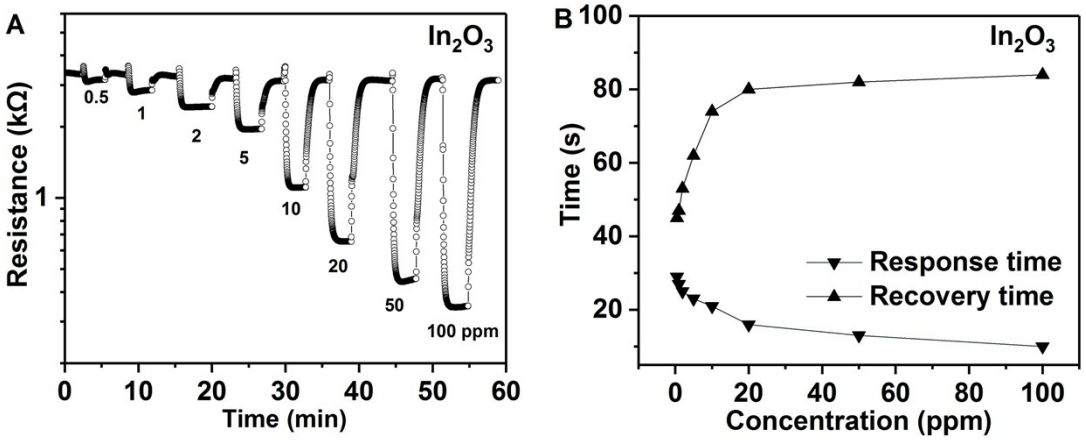

Figure S6 (A) The dynamic resistance of the In_2O_3 sensor toward various concentration of formaldehyde at 120 °C, (B) Response time and recover time of 5Y-In_2O_3 toward formaldehyde at 120 °C.

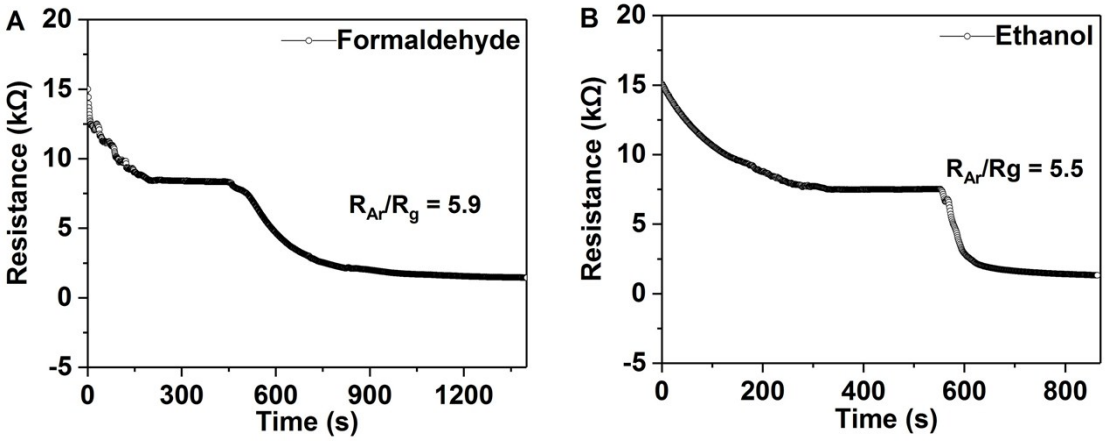

Figure S7 In argon atmosphere, the responses of 5Y-In_2O_3 sensor to 100 ppm (A) formaldehyde and (B) ethanol at 120 °C.

Table S1 Comparison of 5Y-In_2O_3 and In_2O_3-based sensing materials reported in literature for formaldehyde sensing performance**.**

Sening material	Formaldehyde concentration	Response time (s)	Recovery time (s)	Operating Temperature	Response	Reference
5Y-In_2O_3	**100 ppm**	**1**	105	120 °C	91.7	This work
In_2O_3/1% Co	10 ppm	60	120	130 °C	23.2	1
$Al_{0.15}In_{1.85}O_3$	100 ppm	2	103	150 °C	60.3	2
$Ga_{0.6}In_{1.4}O_3$	100 ppm	1	70	150 °C	52.4	3
Au-loaded In_2O_3	100 ppm	3	8	240 °C	37	4
1 at% Pt-In_2O_3	10 ppm	2	51	120 °C	26	5
Ag-loaded In2O3	20 ppm	0.9	14	240 °C	113	6
In_2O_3-H10	100 ppm	100	70	230 °C	80	7

Table S2 BET specific surface area (S_{BET}), pore volume and averaage pore size distribution of 5Y-In_2O_3 and In_2O_3 were determined by N_2 adsorption-desorption measurement.

Sample	S_{BET} (m^2/g)	Average pore size (nm)	pore volume (cm^3/g)
In_2O_3	18	13	0.041
5Y-In_2O_3	19	14	0.044

Table S3 The binding energy and relative percentage of oxygen species in In_2O_3 and 5Y-In_2O_3 according to their fitted O 1s XPS Spectra.

Sample	Oxygen species	Binding energy (eV)	Relative percentage (%)
In_2O_3	Chemisorbed oxygen	531.9	22
	Oxygen vacancy	530.5	24
	Lattice oxygen	529.8	54
5Y-In_2O_3	Chemisorbed oxygen	532.2	34
	Oxygen vacancy	530.8	36
	Lattice oxygen	530.1	30

Table S4 Work functions and Fermi levels of RE-In_2O_3 and In_2O_3, and the responses of RE-In_2O_3 and In_2O_3 sensor to 100 ppm formaldehyde at 120 °C.

Sample	Work function (eV)	Fermi level (eV)	Responses (R_a/R_g)
In_2O_3	5.08	-5.08	12.6
5Y-In_2O_3	4.94	-4.94	91.7
5La-In_2O_3	4.95	-4.95	52.4
5Nd-In_2O_3	4.97	-4.97	49.1
5Ho-In_2O_3	4.94	-4.94	41.4
5Tm-In_2O_3	4.93	-4.93	40.5

References

1 Z.H. Wang, C. L. Hou, Q. M. De, F. B. Gu, D. M. Han, One-Step Synthesis of Co-Doped In_2O_3 Nanorods for High Response of Formaldehyde Sensor at Low Temperature, *Acs Sensors,* 2018, **3**, 468-475.

2 H. Chen, Y. Zhao, L. Shi, G. D. Li, L. Sun and X.X. Zou, Revealing the Relationship between Energy Level and Gas Sensing Performance in Heteroatom-Doped Semiconducting Nanostructures, *ACS Appl. Mater. Interfaces,* 2018, **10**, 29795-29804.

3 H. Chen, J. Hu, G. D. Li, Q. Gao, C. Wei and X. X. Zou, Porous Ga-In Bimetallic Oxide Nanofibers with Controllable Structures for Ultrasensitive and Selective Detection of Formaldehyde, *ACS Appl. Mater. Interfaces,* 2017, **9**, 4692-4700.

4 S. Zhang, P. Song, J. Li, J. Zhang, Z. X. Yang, Q. Wang, Facile approach to prepare hierarchical Au-loaded In_2O_3 porous nanocubes and their enhanced sensing performance towards formaldehyde, *Sens. Actuators, B*, 2017, **241**, 1130-1138.

5 R. J. Ma, X. Zhao, X. X. Zou, G. D. Li, Enhanced formaldehyde sensing performance at ppb level with Pt-doped nanosheet-assembled In_2O_3 hollow microspheres, *J. Alloy. Compd.* 2018, **732**, 863-870.

6 S. M. Wang, B. X. Xiao, T. Y. Yang, P. Wang, C. H. Xiao, Z. F. Li, R. Zhao, M. Z. Zhang, Enhanced HCHO gas sensing properties by Ag-loaded sunflower-like In_2O_3 hierarchical nanostructures, *J. Mater. Chem. A*, 2014, **2**, 6598-6604.

7 F. B. Gu, C. J. Li, D. M. Han, Z. H. Wang, Manipulating the Defect Structure (V-O) of In_2O_3 Nanoparticles for Enhancement of Formaldehyde Detection, *ACS Appl. Mater. Interfaces,* 2018, **10**, 933-942.